HIGH-GRADIENT NORMAL-CONDUCTING RADIO-FREQUENCY PHOTOINJECTOR SYSTEM FOR THE SINCROTRONE TRIESTE

L. Faillace[#], R. Agustsson, P. Frigola, A. Verma, Radiabeam Technologies LLC, CA, USA
H. Badakov, A. Fukasawa, J. Rosenzweig, A. Yakub, Department of Physics and Astronomy,
UCLA CA, USA
F. Cianciosi, P. Craievich, M. Trovo', Sincrotrone Trieste, Italy

Abstract

Radiabeam Technologies, in collaboration with UCLA, presents the development of a high gradient normal conducting radio frequency (NCRF) 1.6 cell photoinjector system, termed the Fermi Gun II, for the Sincrotrone Trieste (ST) facility. Designed to operate with a 120MV/m accelerating gradient, this single feed, fat lipped racetrack coupler design is modeled after the LCLS photoinjector with a novel demountable cathode which permits cost effective cathode exchange. Full overview of the project to date, installation and high-power RF conditioning at Sincrotrone Trieste will be discussed along with basic, design, engineering and manufacturing.

INTRODUCTION

Radiabeam is currently involved in the development of new technology aimed at high average power operation for a NCRF electron gun system, the FERMI II RF Gun, for the Sincrotrone Trieste facility operating at the frequency of 2.99801GHz.

The gun design was originally based on the UCLA-University of Roma-INFN-LNF [1] high repetition rate photoinjector for SPARX project, which was based on the LCLS [2,3] version and using a larger radius of curvature in the rounding of the input coupler irises, and by including an enhanced cooling channels system in the most highly dissipative regions in the structure. This basic design was re-optimized by request of ST to use a replaceable cathode for easy exchange of different material samples with a repetition rate >50Hz.

RF GUN DESIGN

The RF design of the Gun has been performed by using the codes SuperFish [4] and HFSS [5]. Figure 1 shows half structure of the RF gun with surface electric field distribution calculated by HFSS. RF power is fed through one waveguide only (top one); the waveguide located 180deg. opposite the input one, a dummy waveguide, forbids the propagation of the electromagnetic field that is below its cutoff value (i.e. the dummy waveguide has a width much smaller than the input one). The main purpose of the second waveguide is to cancel the field dipole component.

Cell Design

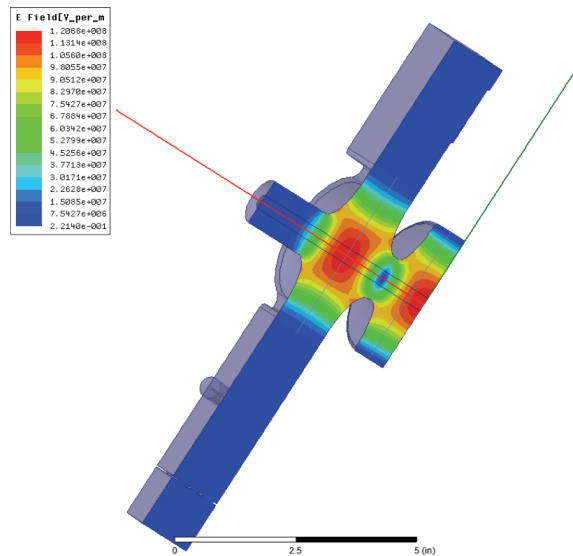The RF cavity shape, as proposed, has several

Figure 1: 3D model used for HFSS simulation. Surface electric field is shown.

innovative electromagnetic features, including Z-coupling and enhanced cell-to-cell coupling to produce higher mode separation, elliptical irises to reduce surface electric field, symmetric couplers for dipole mode minimization, racetrack geometry to minimize quadrupole field components. In contrast to the LCLS gun, which has these features, it is externally fed only by one side, avoiding the need of a power splitter and making the whole assembly much more compact, easier to handle and cost efficient.

In order to calculate the maximum surface electric field, we normalize the on-axis field to 120 MV/m at the cathode. The peak field on the iris is found to be 102 MV/m, below the breakdown safety threshold.

The profile of the simulated axial accelerating electric field is shown in Figure 2.
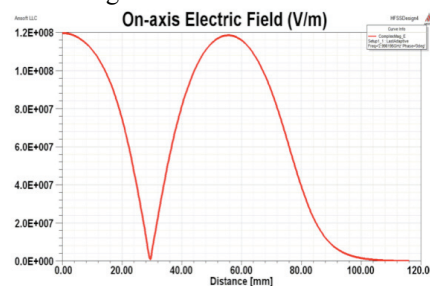

Figure 2: On-axis electric field, from HFSS.

Per usual procedure, a first pass on the RF design was made with SUPERFISH and then HFSS was used to provide a complete picture of the RF performance, including mode frequencies, field balance, quality factor Q, shunt impedance and external coupling.

The design parameters achieved in simulation through this process are summarized below in Table 1.

Table 1: Main RF Parameters.

Parameter	Simulated value
π-mode frequency	2.998 GHz
0-π mode separation	14.2 MHz
Quality factor Q_0	13,750
External coupling β	1.8
Shunt Impedance R_{Shunt}	60.8 MΩ/m
Peak Surface E (120 MV/m @cathode)	102 MV/m
Input power P	<10 MW

Dipole and Quadrupole Component

The dipole and quadrupole components of the RF field have been evaluated using HFSS. The symmetry of the Z-coupling structure guarantees cancellation of the RF dipole component, apart from a negligible (in high-Q standing wave devices) transient from the single-side RF feed. The quadrupole field, on the other hand, is managed by adjusting the "race-track" spacing.

This procedure is intricate, as one must simultaneously optimize cell frequencies, mode separation, field balance, external coupling, and quadrupole strength.

THERMAL ANALYSIS

In the thermal analysis, we assume an overall 50 Hz repetition rate, with a 3μs RF pulse, yielding a duty factor of 1.5E-4 and thus, with 8.8 MW peak power, an average power of P_{avg}=1.32 kW. The water cooling channel placement is as shown in Figure 3, with a flow velocity of 4 m/sec. The water temperature is chosen to be 38°C to optimize thermal gradients, while the ambient laboratory temperature is assumed to be 27°C.
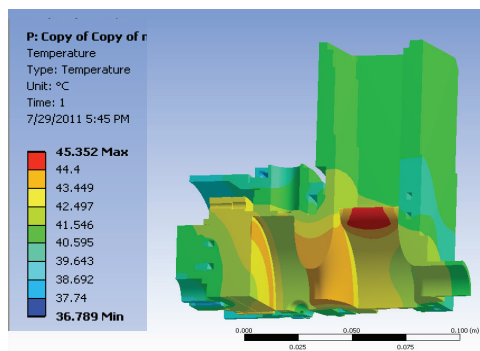

Figure 3: Temperature distribution.

The peak temperature in the structure is < 46°C with only a 2°C gradient. This temperature distribution

produces stresses that have been analyzed consistently in the ANSYS [6] modeling codes. The resultant distortion of the copper structure produces a small change in the resonant frequency of the structure that is easily managed by real-time adjustments in the cooling water temperature, as is used at the LCLS.

GUN FABRICATION, TUNING AND LOW-POWER MEASUREMENTS

One of the crucial features of the Fermi II Gun is represented by the cooling assembly. Cathode cooling is carried out by adapting a straightforward scheme similar to that of the LCLS gun. Nevertheless, the main difference between the LCLS design and the FERMI RF gun II design is the incorporation of an exchangeable cathode system made out of a two-piece part. RadiaBeam has evaluated several different solutions to this request. The final selection and engineering of the cathode system was made during the engineering phase, with input and approval from ST.

The RF Gun was machined in-house and all the brazing cycles at SLAC, followed by final tuning. The Gun after the final brazing step is shown in Figure 4.
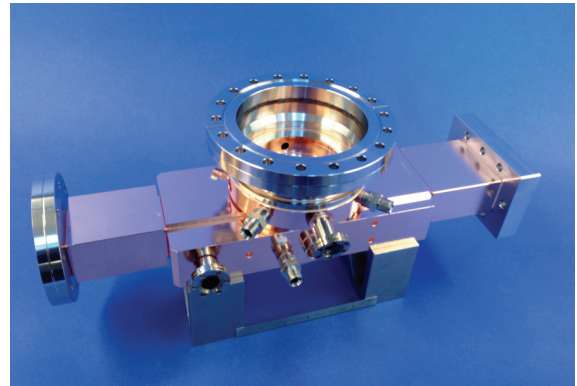

Figure 4: picture of the Fermi II Gun after final brazing.

In order to check the simulated parameters, we performed low-power measurements by using a Vector Network Analyzer (VNA). The comparison is given in table 2, showing good agreement.

Table 2: Comparison between simulations and measurements of the main RF parameters.

	Measurement	**HFSS**
Frequency	2.99801 GHz (19 C, 40% humidity)	2.998GHz
Mode Separation	14.5 MHz	14.2 MHz
Q_0	13,350	13,750
Coupling beta	1.85	1.8

The reflection coefficient at the input RF waveguide is shown in Fig. 5. The tuning frequency was set to 2.99801,

02 Synchrotron Light Sources and FELs

T02 Electron Sources

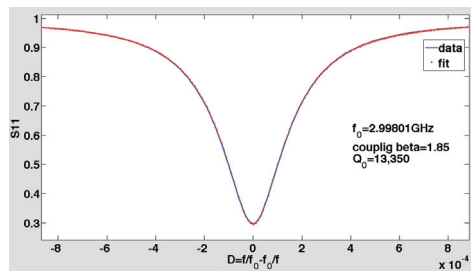at 19°C and 40% humidity (assuming an operating temperature of 38°C).

Figure 5: reflection coefficient. Data (red dots) and fit (blue line).

The balance of the electric field profile was measured by means of the bead-drop procedure and using a 2mm dielectric spherical bead. The good agreement between data and fit is given in Fig. 6.
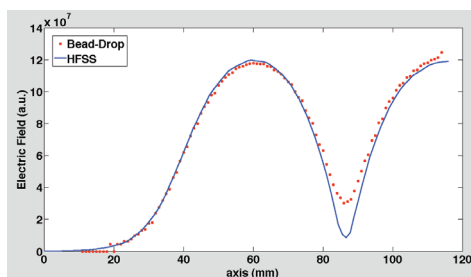

Figure 6: On-axis electric field profile. Data (red dots) and fit (blue line).

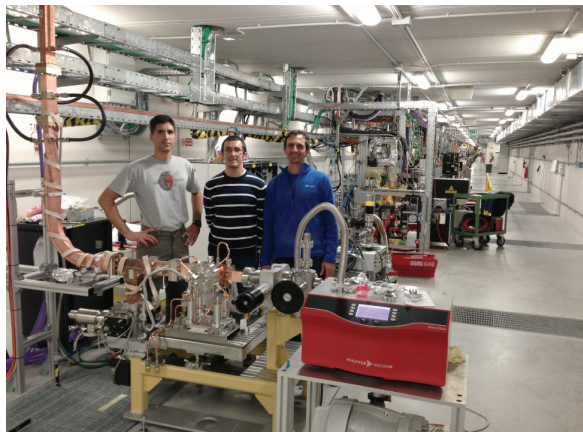## INSTALLATION AND HIGH-POWER RF CONDITIONING

Figure 7: Fermi II gun installed in the test area (Fermi FEL tunnel).

The Fermi II Gun Installation started in Trieste on January 4th 2013. The gun was brought under vacuum in a test area (see Fig. 7) to check if any leaks were present as well as the frequency shift that resulted to be about 800 kHz, as expected.

A dedicated area for high-power gun testing is located behind the current RF gun station. The Fermi II gun was installed in this area to start high-power conditioning.

The power signals (forward, reflected and probe), read from an oscilloscope, are plotted in Fig. 8.
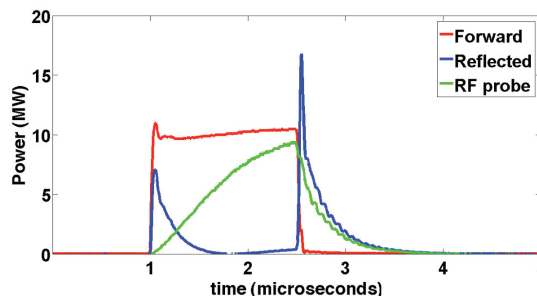

Figure 8: Power forms of the RF signals.

The input power was raised up to 11MW and a repetition rate of 50Hz. The conditioning between 10Hz and 50Hz, given in the chart in Fig. 9, led to a temperature variation of only 2°C. The vacuum base level was $2.4 \; 10^{-9}$ mbars.
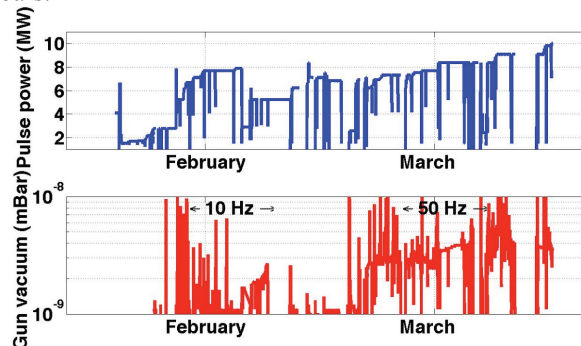

Figure 9: Monitoring of the high-power conditioning and vacuum levels.

CONCLUSIONS

We have presented the RF design, fabrication and high-power RF conditioning of the Fermi II RF Gun. Innovative features to the class of RF Guns, such as elliptical irises and an exchangeable cathode system, improve the performance of this gun in terms of power handling and robustness. The removable cathode assembly showed good thermal performance even at 50Hz.

REFERENCES

[1] L. Faillace *et al.,* " An Ultra-high repetition rate S-band RF Gun", FEL Conference 2008

[2] C.Limborg *et al.,* "RF Design of the LCLS Gun", LCLS Technical Note LCLS-TN-05-3 (Stanford,2005).

[3] D.H. Dowell *et al.,* "The development of the Linac Coherent Light Source RF Gun", SLAC Menlo Park CA, published in the ICFA Beam Dynamics Newsletter No.46

[4] http://laacg1.lanl.gov/laacg/

[5] http://www.ansoft.com/products/hf/hfss

[6] http://www.ansys.com